# Nanoscale

## Accepted Manuscript

ROYAL SOCIETY OF CHEMISTRY

www.rsc.org/nanoscale

# Nanoscale

**PAPER**

# Smart conducting polymer composites having zero temperature coefficient of resistance

**Kunmo Chu,[a] Sung-Chul Lee,[a] Sangeui Lee,[a] Dongearn Kim,[b] Changyoul Moon,[a] and Sung-Hoon Park[*a]**

Zero temperature coefficient of resistance (TCR) is essential for the precise control of temperature in heating element and sensor applications. Many studies have focused on developing zero-TCR systems with inorganic compound; however, very few have dealt with developing zero-TCR systems with polymeric materials. Composite systems with a polymer matrix and conducting filler show either negative
10 (NTC) or positive temperature coefficient (PTC) of resistance, depending on several factors, e.g., the polymer nature and the filler shape. In this study, we developed a hybrid conducting zero-TCR composite having self-heating properties for thermal stability and reliable temperature control. The bi-layer composites consisted of a carbon nanotube (CNT)-based layer having a NTC of resistance and a carbon black (CB)-based layer having a PTC of resistance which was in direct contact with electrodes to stabilize
15 the electrical resistance change during electric Joule heating. The composite showed nearly constant resistance values with less than 2% deviation of the normalized resistance until 200 °C. The CB layer worked both as a buffer and as a distributor layer against the current flow from an applied voltage. This behavior, which was confirmed both experimentally and theoretically, has been rarely reported for polymer-based composite systems.

## Introduction

20 Polymer composites containing conducting fillers such as carbon-based materials and metal fibers have been extensively investigated for multi-functional applications owing to their light weight and processibility.[1-5] In particular, they are a practical
25 choice of material in heat-related applications such as in patternable micro heaters, temperature sensors, heating glasses for vehicles, thermoelectric devices, water heaters, and flexible de-icing units.[6-9] By the electric Joule heating (resistive heating) of conducting composites, electrical energy can be converted into
30 heat energy easily and quantitatively. In general, composites that

45 exhibit high conductivity and low heat capacity are ideal for rapid heating applications. Carbon-based materials such as carbon black (CB) and fibers have previously been used in conducting polymer composites;[10] however, their widespread use is limited because there exists an upper limit to their loading capability,
50 beyond which embrittlement occurs. Therefore, carbon nanotubes (CNTs) are more attractive candidates as filler materials in composites, primarily because of their high aspect ratio coupled with high electrical and thermal conductivities, which could be as high as $10^6$ S/m and 6600 W/mK, respectively.[11-13] These
55 properties enable electrical percolation with very small volumes of nanotubes.[14]

However, issues with regard to the temperature coefficient of resistance (TCR) have to be addressed to enable the practical use of conducting polymer composites for heat-related applications.
60 The term TCR is used to indicate the increment or reduction in electrical resistance caused by a temperature increment in the composite, which can cause serious safety problems and inaccuracies. The increase in resistivity with increasing temperature is described by a positive temperature coefficient
65 (PTC) of resistance, while the decrease in resistivity with increase in temperature is described by a negative temperature coefficient (NTC) of resistance. For many electronic device applications, it is highly desirable to have resistors with a small or zero TCR. For

*[a] Samsung Advanced Institute of Technology, Suwon, 443-803, Korea. Tel:+82-70-4114-2219; E-mail: leo.park@samsung.com*
*[b] Korean Institute of Industrial Technology, Incheon, 406-840, Korea*

35 † Electronic Supplementary Information (ESI) available: Normalized resistance as a function of increasing temperature for CNTs with different aspect ratio, other configurations of the bi-layered composite with the corresponding circuit diagrams, SEM image of CNT/PDMS composite with low resolution and dependence of DC conductivity on the number of
40 three roll passes, numerically calculated normalized resistance of the bi-layer composite with different thickness ratio, streamline and arrow plots of the current densities of the bi-layer composites with other configurations. See DOI: 10.1039/b000000x/

example, in the case of composites exhibiting a NTC of resistance, the composites can be overheated and burned by excessive current flow originating from a constant supplied voltage. In circuit systems, this can cause thermal runaway,
5 which destroys the resistor and/or other parts of the circuit. On the other hand, in the case of composites exhibiting a PTC of resistance, they can be used as current limiter and over current protector.[15] However, along with the lack of reproducibility due to irregular structure changes in heating/cooling cycles, it is
10 impossible to reach a high temperature through an electric Joule heating owing to the marked increment in electrical resistance.[16] Therefore, zero TCR is necessary for the precise control of temperature in heating element and sensor applications. While many studies have focused on developing inorganic systems such
15 as metal alloy and antiperovskite systems with zero TCR,[17-20] very few studies have focused on polymer-based systems with zero TCR.[21] In general, most conductive materials used as fillers including CNTs and CB typically exhibit a PTC of resistance. [19] However, composite systems consisting of a polymer matrix and
20 a conducting filler may show negative or positive temperature coefficient of resistance depending on several factors such as the nature of the polymer (determined by the thermal expansion coefficient, melting point, stiffness, and glass transition temperature of the polymer) and the shape of the filler
25 (determined by the particle size and aspect ratio).[10,16,22-25] In addition, although several researchers have examined the electrical behavior of CNT devices or composites under heating or cooling for sensor applications,[23,26] the mechanisms responsible for polymer composites exhibiting a NTC or PTC of
30 resistance remain unclear, even though several mechanisms have been proposed. Consequently, in this study, we have developed a hybrid conducting composite with zero TCR to achieve thermal stability and reliable temperature control. The composite consisted of two layers with different types of TCR (negative and
35 positive), as shown Fig. 1. The CB-based layer exhibiting PTC of resistance, which was in direct contact with electrode, was combined with the CNT-based layer showing NTC of resistance to stabilize the change of electrical resistance during electric heating. In this system, the CB layer functioned as both a buffer
40 and a distributor layer against the current flow originating from an applied voltage, which was confirmed both experimentally and theoretically. Such a behavior is rarely reported in polymer-based composite systems.

## Experimental
45

### Sample preparation

For fabricating the bi-layer composites, PDMS (Dow 5050 liquid silicone elastomer base, Dow Corning), multiwalled carbon nanotubes (MWNTs) (Nanocyl, outer diameter = 10 nm and
50 length = 10 μm), and carbon blacks (Model: 484164, Aldrich, particle diameter = 2–12 μm) were used. To ensure effective mixing and dispersion of the highly entangled CNTs and CBs within the polymer matrix, premixing (paste mixer, DAE HWA TECH, PDM-1k) and a three-roll milling technique (Ceramic 3
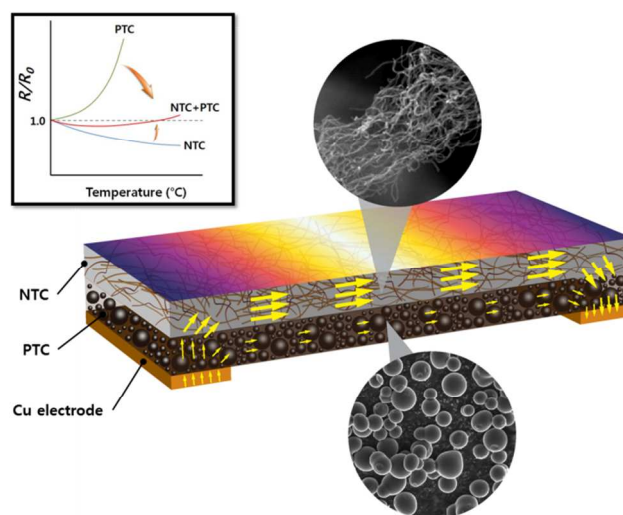55 roll mill, Inoue Mfg. Inc.) were used. Briefly, CNTs (or CBs) and



**Fig. 1** Scheme representation of the zero TCR bi-layer composite consisting the CB-based composite (PTC) layer and the CNT-based composite (NTC) layer. The CB-based composite (PTC)
60 layer was in direct contact with the Cu electrode to split/control the current flow. The inset shows the concept of TCR compensated heating achieved by using two parallel layers.

the PDMS-based elastomer were mixed using the paste mixer for
65 1 minute to form a paste. Then, the pastes were milled using the three-roll miller with gradually decreasing gaps between the rolls for several minutes. Using a film applicator (Micrometer film applicator, Mitutoyo), each of the CNT and CB pastes was processed into a film with the desired thickness on a glass plate.
70 Then, the two glass plates (containing the CNT and CB pastes) were folded and slightly pressed without physical deformation. Subsequently, a convection oven (120 °C, 30 minutes) was used for curing the plates to fabricate the bi-layer composites film.

75 ### Characterization

The morphology and the structural features of the bi-layer composites were characterized by an optical microscope (Olympus) and by scanning electron microscopy (SEM: Hitachi, Field Emission SEM, S-4500 XL30). To evaluate the electric
80 heating behavior of the bi-layer composites, direct current was applied to the samples (National Instruments, NI PXI-1033). Then, the thermal infrared images were recorded using a thermal infrared camera (Advanced Thermo, TVS-500). The composites were sliced into a rectangular ($5 \times 30$ mm$^2$) samples with a
85 thickness of around 0.5 mm. The composite was suspended between copper conducting tape/glass electrodes. To ensure good electrical contacts, conductive silver paste was used between the samples and the copper conducting tape. The heater output characteristics of the composites were evaluated by measuring the
90 change in the resistance and the temperature of the heater at an applied DC voltage. The steady-state current distribution of the bi-layer composites were calculated by applying Ohm's law. The variation of temperature along the thickness was neglected.

95 ## Results and discussion

### Characterization of polymer composites having NTC or PTC of resistance

In general, for thermosetting polymers containing micrometer sized fillers such as carbon black (CB), carbon fiber, or metallic particles, the resistivity of the composites progressively increase with increase in temperature (PTC effect) owing to the difference in the thermal expansion of the polymer and the conducting filler (for CB: ~ $1.2 * 10^{-6}$ $K^{-1}$, for CNT: $-1\sim7 * 10^{-6}$ $K^{-1}$, for PDMS: ~ $3.1 * 10^{-4}$ $K^{-1}$).[10,16,27,28] When the gap between the conducting fillers is increased during heating, tunneling or hopping of charge carriers could reduce, resulting in an increase in the resistivity of the composites. On the other hand, the increase in resistivity can be moderated at higher filler concentrations due to the higher probability of tunneling effect though the presence of larger and closely packed conducting fillers contacts. However, besides the existence of a limit of the loading capacity, composites consisting of spherical fillers cannot reach high temperature ranges. For example, when the CB-based polydimethylsiloxane (PDMS) composite shown in Fig. 2 (a) (with a CB weight fraction of 60%) was subjected to electric Joule heating by applying voltage, the resistance began to increase with an increase in the temperature gradually, as shown Fig. 3 (a). Although it showed relatively adequate electrical conductivity (30 S/m) at room temperature, resistance of CB composite sharply increased as the temperature approached 50 °C (PTC behavior). Consequently, the increased normalized resistance change ($R/R_0$) of the CB-based composite was about 1000% temperature under an applied DC voltage of 16 V. Furthermore, the temperature of the CB-composite did not increase beyond 50 °C even with further increasing voltage.

Unlike the CB-based composite, the composite consisting of high aspect ratio fillers such as CNTs shown in Fig. 2 (b) (with CNT weight fraction of 12% and conductivity of 250 S/m) appeared to exhibit a NTC of resistance by applying voltage, as shown in Fig. 3 (b), although the CNTs themselves typically show a PTC of resistance.[22] The initial normalized resistance decreased up to 60% at 200 °C under an applied DC voltage of 9 V. This difference existed because in the composite system, which consisted of both insulating regions (polymer matrix) and long conducting regions (CNTs), the interconnection contacts between the high aspect ratio CNTs prevailed over the metallic filler (PTC) properties during thermal expansion, resulting in a NTC of resistance.[23,27-30] In addition, the degree of the NTC of resistance originating from the interconnection resistance between the CNTs could be enhanced by using higher aspect ratio CNTs, as shown in the Fig. S1†. CNT-based composites with higher aspect ratio CNTs of the same weight fraction showed much lower normalized resistance by increasing temperature. Therefore, even if the CNTs are ideal fillers from the viewpoints of achieving high conductivity at very low loading and attaining rapid heating,[24] the dramatic decrease in the resistance is inappropriate for the fabrication of safe heating elements or accurate heat sensors because of the excessive current flow. In addition, simple mixing of CB (causing a PTC of resistance) and CNTs (causing a NTC of resistance) in a polymer was unhelpful in achieving zero TCR composites.[31] For example, analysis and control of composites consisting of two heterogeneous fillers is difficult due to its sensitivity and complexity.
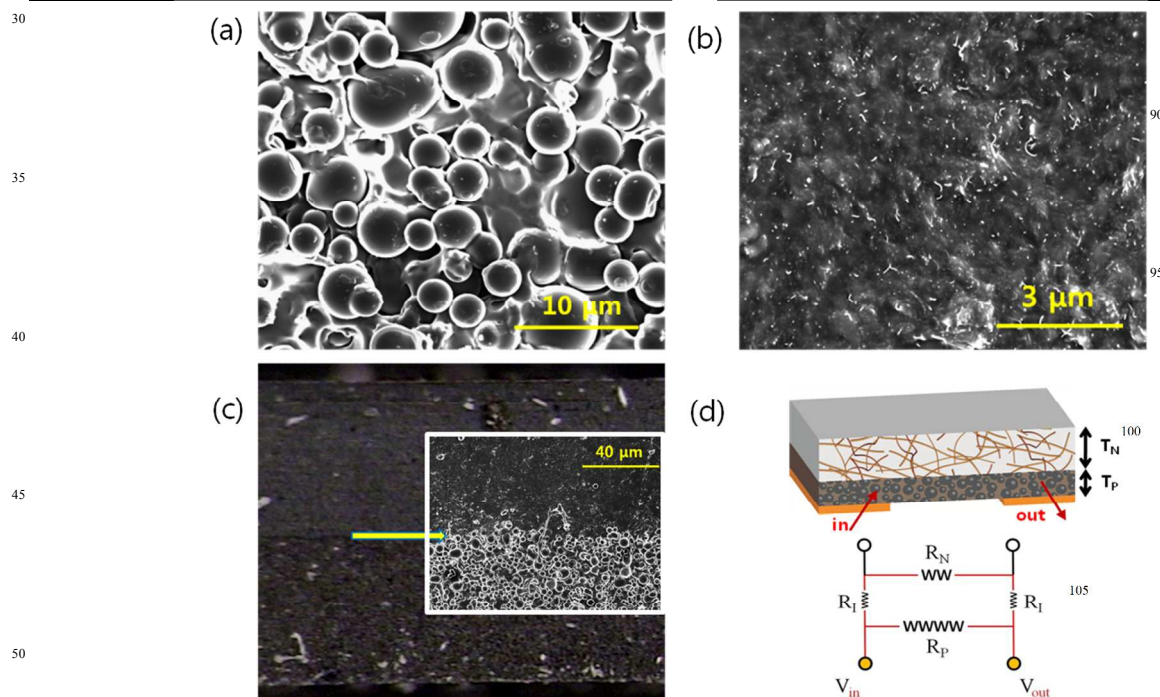


**Fig. 2** SEM images indicating uniform dispersion of (a) CBs and (b) CNTs in the PDMS matrix. (c) Optical microscope image of the bi-layer (CNT-based layer/CB-based layer) composite. The inset shows the interfacial region between the CB/PDMS and the CNT/PDMS layers. (d) Circuit diagram of the bi-layer composite. ($T_N$: thickness of the NTC layer, $T_P$: thickness of the PTC layer, $R_N$: resistance of the NTC layer, $R_P$: resistance of the PTC layer, and $P_I$: contact resistance between the CB/PDMS layer and the CNT/PDMS layer)
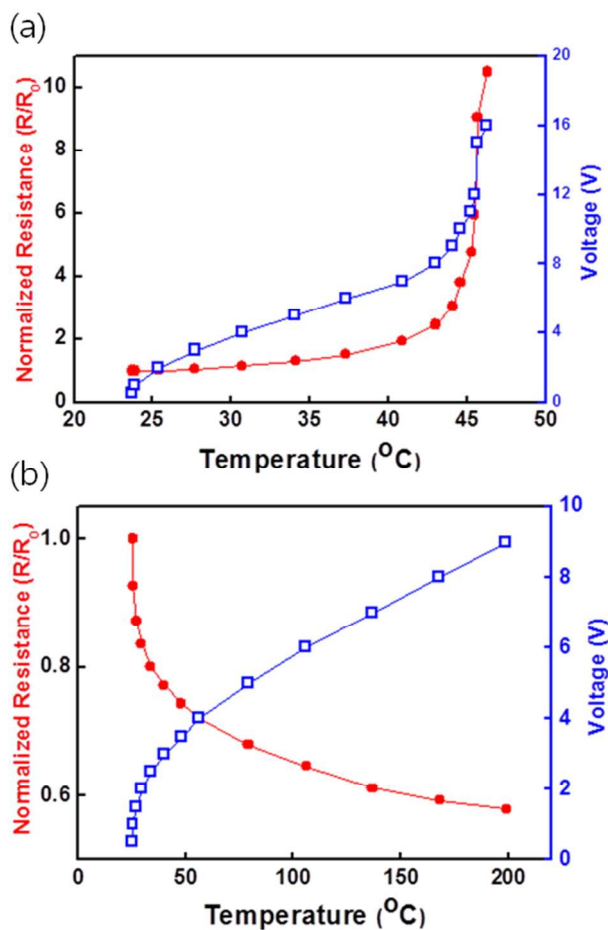
**Fig. 3** (a) Resistance-temperature plot of the CB/PDMS composite showing a PTC of resistance and (b) Resistance-temperature plot of the CNT/PDMS composite showing a NTC of resistance. In the CB/PDMS composite, the normalized resistance increased markedly with increasing voltage. In the CNT/PDMS composite, the normalized resistance decreased rapidly with increase in voltage.

**Synthesis and chracterization of bi-layer composites having zero TCR**

To achieve zero TCR polymer-based composites, we designed a hybrid composite structure consisting of two layers i.e., a CB-based and a CNT-based composite layer, in parallel. The schematic of the bi-layer composite for zero TCR is shown in Fig. 1. In this configuration, the current from the Cu electrode is distributed through the CB-based composite (PTC) layer and the CNT-based composite (NTC) layer. Combining these two composites is estimated to lead to zero TCR, as shown in inset of Fig. 1, which can be achieved by the compensation of PTC and NTC of resistance. A simple circuit diagram of the parallel bi-layer composite, which could be defined as a function of the PTC layer and the NTC layer, is shown in Fig. 2 (d), and its resistance could be represented by the equation shown below.

$$R_T = \frac{2R_P R_I + R_N R_P}{(R_N + R_P) + 2R_I} \tag{1}$$

Where, $R_T$ is the total resistance of the bi-layer composite, $R_P$ is the resistance of the composite showing a PTC of resistance (i.e., the CB-based composite), $R_N$ is resistance of the composite

showing NTC of resistance (CNT-based composite), and $R_I$ is the interfacial resistance between the two composite layers. The other possible configurations of the two parallel composites are shown with circuit diagrams (Fig. S2†). The key points in the design of the zero TCR composite are as follows: (1) The layer showing the PTC of resistance with higher resistance should be in direct contact with each Cu electrode, which controls the current flow to the lower resistance layer and (2) The layer showing a relatively small change in resistance (PTC: +1000% vs NTC: -60%) should be selected as the main current flow layer during the entire course of heating as shown Fig. 1. Lastly, (3) we have observed that the dominant change in resistance of both PTC and NTC composites occurred during initial heating from room temperature to 50 °C as shown in Fig. 3 (a) and (b). The configuration shown in Fig. 2 (d) is fairly satisfied above conditions to achieve zero TCR during heating up to 200 °C. Considering resistance values of each PTC and NTC layer from Fig. 3 (a) and (b) are temperature dependent parameters with certain dimension (i.e., 30 and 250 S/m for electrical conductivity of PTC and NTC layer at room temperature, 2.9 and 431.8 S/m at 200 °C), the terms $R_P$ and $R_N$ in equation (1) were found to be a function of the thickness of the layers and the temperature at particular width. In this case, reliable electrical conductivity of CB and CNT-based composite can be attained through three-roll milling process.[32] During three-roll milling, shear forces created by three horizontally positioned rolls rotating in opposite directions and at different speeds disentangle the heavily entangled CNTs. The method can uniformly shear the entire volume of material resulting evenly dispersed CNTs within the whole polymer matrix (Fig. S3†). In addition, very low deviation (within 2%) of electrical conductivity could be achieved through optimal three roll milling time (Fig. S3†). However, at the same time, slight decrement of conductivity is observed due to shortening of CNTs without disrupting the basic morphology of the carbon nanotubes after three roll milling process (Fig. S3†).[33-35] Therefore, it can be concluded that zero TCR can be achieved by carefully controlling the ratio of the thickness of the two layers ($T_P/T_N$, where $T_N$: thickness of NTC layer and $T_P$: thickness of PTC layer) under a certain temperature range. The required $T_P/T_N$ for constant $R_T$ ($R_T/R_{T0}$ ~1) between room temperature and 200 °C can be determined from numerical calculation, which will subsequently be compared with the experimental results. For the PTC layer, the resistance above 50°C is (Fig. 3 (a)) almost an insulator. Therefore, we assumed resistance of PTC layer over 50°C is unlimited (∞). Thus, from Eq.(1), $R_T$ is converged into $R_N$ for over 50°C. Bi-layer composites with different $T_P/T_N$ ratio (0.3, 0.85, and 1.5) were synthesized to determine the resistivity-temperature behavior, as shown in Fig. 4 (a). For example, when $T_P/T_N$ = 0.85, the total thickness of the bi-layer composite (CB layer ~ 460 μm and CNT layer ~ 540 μm) was about 1000 μm. In synthesis of bi-layer composites, controlling the ratio of the thicknesses of the two layers and relatively good adhesion can be easily achieved by using a film applicator before the curing process. Fig. 2(c) shows the optical image of the bi-layer composite with the desired ratio of the two layer thicknesses. The SEM image of the interfacial region between the CB/PDMS and CNT/PDMS layers is shown in the inset of Fig. 2(c). In this bi-
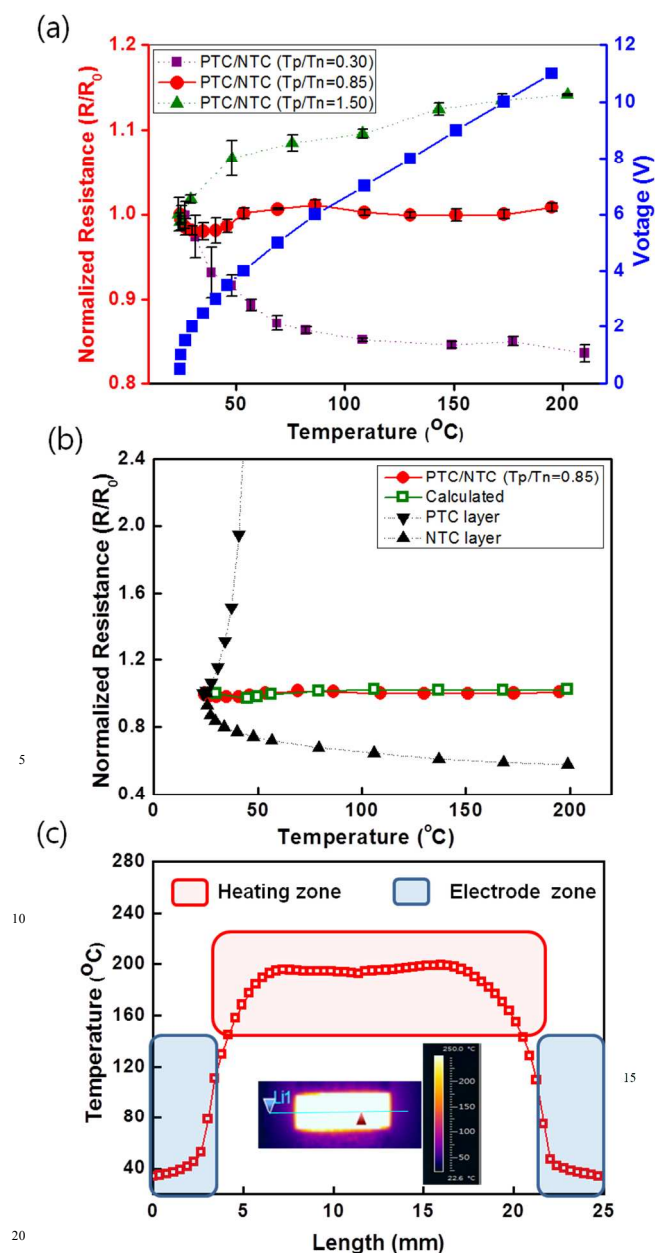
**Fig. 4 (a)** Resistance-temperature plot of the bi-layer composite with different thickness ratios ($T_P/T_N$ = 0.3, 0.85, and 1.5). When $T_P/T_N$ = 0.85, the bi-layer composite showed stable zero TCR behavior with less than 2% deviation of the normalized resistance. (b) Comparison of the resistance-temperature plots of the bi-layer composite, CB, and CNT composites with the calculated value, which shows significant improvement of zero TCR. (c) Temperature profile of the bi-layer composite (at $T_P/T_N$ = 0.85) between the two Cu electrodes under an applied DC voltage of 11 V. Only the bi-layer composite between the two electrodes showed electric Joule heating, resulting in a low temperature profile at the electrode parts.

layer composite, both layer were made with same polymer matrix and contacted firmly before they were cured to secure interfacial adhesion between the two layers. Therefore, we assumed $R_I \ll R_N$ or $R_P$. When $T_P/T_N$ = 0.30 (and 1.5) in Fig. 4 (a), the

normalized resistance decreased (increased) with increase in temperature, resulting in -17% (+11%) change in resistance.

However, a constant normalized resistance was achieved for $T_P/T_N$ = 0.85 until 200 °C when voltage was increased to 0 to 11V, which is an entirely different behavior when compared with the CB and CNT composites shown in Fig. 3 (a) and (b). These behaviors were in agreement with the calculated results (Fig. S4†). In Fig. 4 (b), the deviation of the normalized resistance of the bi-layer composite was less than 2%, in contrast to the significant change in resistance observed in the CB composite (+1000%) and the CNT composite (-60%) layers. The 2% deviation is possibly attributed to the interfacial resistance between two layers, and the values successfully matched with the calculated results as shown Fig. 4 (b). To demonstrate the durability and repeatability, electric heating cycling test has been conducted in the Supporting Information (Fig. S5†). During 50 hours (up to 3000 cycles), the bi-layer composite showed nearly constant resistance with less than 3% deviation. In addition, after the test, there were no mechanical and thermal distortion attributing to elastic properties of PDMS matrix. The temperature profile of the bi-layer composite with $T_P/T_N$ = 0.85 is shown in Fig. 4 (c). The temperature of the surface was 200 °C in most areas between the electrodes by applying a DC voltage of 11V, while the electrode parts showed relatively low temperatures that were lower than 40 °C. The IR camera images (inset in Fig. 4 (c)) confirmed the temperature uniformity during heating.

**Interpretation of bi-layer composites with varying thicknesses and temperatures**

The compensated resistance of the zero TCR composite with a certain thickness at a particular temperature could be interpreted
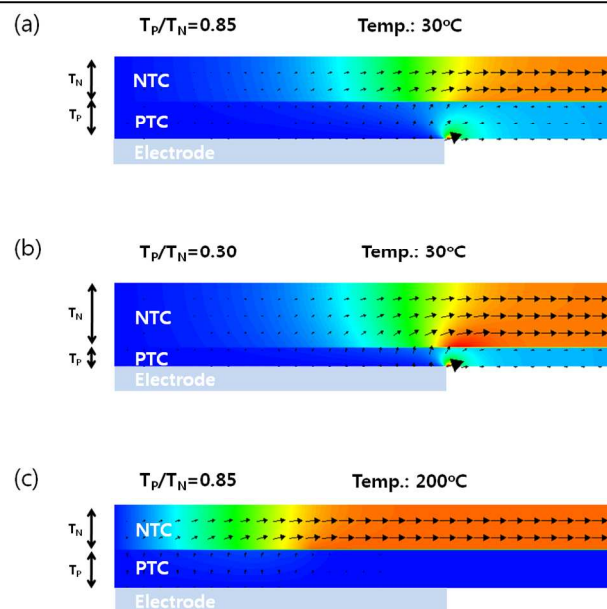


**Fig. 5** Streamline and arrow plots of the current densities in the bi-layer composites with varying thicknesses and temperatures at a voltage of 11 V (a) $T_P/T_N$ = 0.85 and (b) $T_P/T_N$ = 0.3 at room temperature. (c) $T_P/T_N$ = 0.85 at 200 °C.
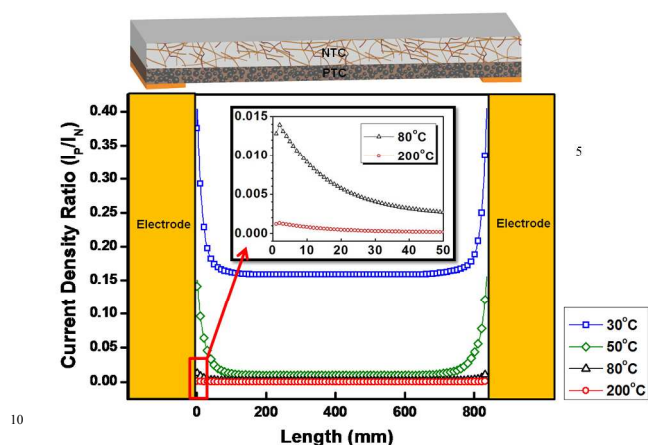
**Fig. 6** Current density ratio ($I_P/I_N$) of the bi-layer composite between two electrodes at various temperatures. By increasing the temperature, the $I_P/I_N$ approached zero, indicating the dominant current flow observed in the NTC layer at higher temperature. The inset shows the magnified images of $I_P/I_N$ at 80 °C and 200 °C. ($I_P$: current in the PTC layer originating from an applied voltage, $I_N$: current in the NTC layer originating from an applied voltage)

through the simulation of the micro-structural development, and the current distribution of bi-layer composites were calculated by Ohm's law.[36,37] Ohm's law is defined in its simplest form as $J = \sigma \cdot E = (1/resistivity) \cdot (V/d)$ (resistivity is a function of temperature), where J is the current density at a given location in a resistive material, E is the electric field at that location, and σ is conductivity, which is a material dependent parameter. Consequently, the streamline and arrow plots of the current densities with different thicknesses and at various temperatures at a voltage of 11 V are shown in Fig. 5 (a)–(c). The streamlines and arrows indicate current flow directions and paths, and the arrow lengths are proportional to the current density. In addition, temperature profiles of the bi-layer composite as shown Fig. 4 (c) was used to determine the streamline and arrow plots of the current densities. In the bi-layer configuration, the Cu electrode was directly connected to the layer exhibiting PTC of resistance and the current flow could split from the layer showing PTC to that showing NTC or remain in the PTC layer only, based on equation (1), and the portion of the current in the two layers depends on the ratio of the two layers thickness ($T_P/T_N$). As shown in Fig. 5(a) and (b), the current entered the PTC layer mainly from the edge of the electrode because the current path is the shortest when the current flow is between the two electrodes.[36-38] In addition, the current density of the NTC layer increased with the decrease in the thickness of the PTC ($T_P$) layer at 30 °C. For this case, the relative thickness ratio of the NTC and PTC layers ($T_P/T_N$) was changed from 0.85 to 0.30. Meanwhile, the temperature also exerted a dramatic influence on the current density ratio between the two layers. As shown Fig. 5 (c), when the bi-layer composite was heated to 200 °C with $T_P/T_N$ = 0.85, the current density of the NTC layer increased, indicating that most of the current flowed through the NTC layer because of the sharp increase in the resistance of the PTC layer. Interestingly, in this case, the current entering the PTC layer was not from the edge point of the electrode and was away from the edge side

which is different behavior from Fig. 5 (a) and (b). When voltage was applied between the two electrodes of the bi-layer composite, only the bi-layer composite part between Cu electrodes is responsible for the Joule heating, resulting in the temperature profile of the bi-layer composite as shown in Fig. 4(c). Therefore, the lower temperature (< 40 °C) of the electrode contact zone enabled current flow in the PTC layer to NTC layer during heating up to 200 °C, also causing left drift of current density distribution to the edge side of electrode as shown in Fig. 5(c). For example, if the temperature of the electrode contact zone was over 50°C, the current flow from the PTC to NTC layer was hampered because of the significant increase in the resistance of the PTC layer. In addition, the streamline and arrow plots of the current densities of the bi-layer composites with other configurations shown in Fig. S6† were inefficient for zero TCR because of the dominant NTC behavior at room temperature and 200 °C.

Fig. 6 shows the distribution of the current density ratios of the bi-layer composite ($I_P/I_N$) between the electrodes ($I_P$: current density of PTC layer/ $I_N$: current density of NTC layer) for $T_P/T_N$ = 0.85 at various temperatures derived from Fig. 5 (a) and (c) to further understanding electron transport behavior of bi-layer composite during heating. Both NTC and PTC layers, dramatic decrement were occurred until 50~60°C as shown Fig. 3(a) and (b), therefore it is critical to split current density ratio into PTC and NTC layer during initial heating. In Fig. 6, $I_P/I_N$ significantly decreased until 50 °C indicating that most of the current flowed in the NTC layer at high temperature range while current density efficiently split into PTC and NTC layer at low temperature range (i.e., $I_P/I_N$ ~ 0 at 200°C while $I_P/I_N$ ~ 0.2 at 30°C). Therefore, the bi-layer composite with zero TCR could be systematically designed and was confirmed to be stable up to 200 °C. To the best of our knowledge, this study is the first attempt to obtain stable zero TCR polymer-based composites having self-heating properties which is different from inorganic systems such as metal alloys.

## Conclusions

In summary, we have demonstrated a new hybrid bi-layer zero-TCR composite consisting of stacked layers showing NTC and PTC of resistance. The NTC and PTC layers changed markedly with increasing temperature; however, the designed bi-layer composites showed nearly constant resistance values with less than 2% deviation from the normalized resistance until 200 °C. In this system, the CB-based PTC layer, which was in direct contact with electrodes, functioned as the buffer and the distributor layer against a current flow originating from an applied voltage. The CNT-based NTC layer functioned as the main current flow layer for Joule heating. In addition, with an initial conductivity and width of composites, the trend of the TCR of the bi-layer composites was controlled by changing the relative thickness ratio of the NTC and PTC layers. Consequently, we calculated the optimal thickness ratio of the NTC and PTC layers required to achieve zero TCR, which successfully matched with the experimental values.

A major feature of this hybrid composite is the availability of heating units that show no change in resistance, and this study is one of the first of its kind to attempt to realize zero-TCR polymer-based composites. We envisage that these composites will be extensively used in a wide range of applications as resistors in high precision electric heating systems, flexible resistors in hybrid electronic devices, thermoelectric devices, patternable micro heaters, and as temperature sensors in automobiles.

## Acknowledgements

## References

1. Y. Cheng, S. Lu, H. Zhang, C. Varanasi and J. Liu, *Nano Letters*. 2012, **12**, 4206-4211.

2 K.-Y. Chun, Y. Oh, J. Rho, J.-H. Ahn, Y.-J. Kim, H. R. Choi and S. Baik, *Nature Nanotechnology*. 2010, **5**, 853-857.

3 S. H. Park and P. R. Bandaru, *Polymer*. 2010, **51**, 5071-5077.

4 P. C. Ramamurthy, W. R. Harrell, R. V. Gregory, B. Sadanadan and A. M. Rao, *J. Electrochem. Soc*. 2004, **151**, G502-G504.

5. C. Park, J. H. Kang, J. S. Harrison, R. C. Costen and S. E. Lowther, *Advanced Materials*. 2008, **20**, 2074-2079.

6 Y. H. Yoon, J. W. Song, D. Kim, J. Kim, J. K. Park, S.–K. Oh and C.-S Han, *Adv. Mater*. 2007, **19**, 4284-4287.

7 Y. G. Jeong and G. W. Jeon, *ACS Appl. Mater. Interfaces*. 2013, **5**, 6527-6534.

8 C. Yu, K. Choi, Y. Yin and J. C. Grunlan, *ACS Nano*. 2011, **5**, 7885-7892.

9 S. H. Park, E. H. Cho, J. Sohn, P. Theilmann, K. Chu, S. Lee, Y. Sohn, D. Kim and B. Kim, *Nano Research*. 2013, **6**, 389-398

10 E. S. Park, *Macromol. Mater. Eng*. 2005, **290**, 1213-1219.

11 M. Fujii, X. Zhang, H. Xie, H. Ago, K. Takahashi, T. Ikuta, H. Abe and T. Shimizu, *Phys. Rev. Lett*. 2005, **95**, 065502-065505.

12 S. Berber, Y. K. Kwon and D. Tománek, *Phys. Rev. Lett*. 2000, **84**, 4613-4616.

13 Y. Ryu, L. Yin and C. Yu, *J. Mater. Chem*. 2012, **22**, 6959-6964.

14 S. H. Park, P. Thielemann, P. Asbeck and P. R. Bandaru, *Appl. Phys. Lett*. 2009, **94**, 243111-243113.

15 Y. Xi, H. Ishikawa, Y. Bin and M. Matsuo, *Carbon*. 2004, **42**, 1699-1706.

16 K. P. Sau, T. K. Chaki and D. Khastgir, *Polymer*. 1998, **39**, 6461-6471.

17 L. Ding, C. Wang, L. Chu, J. Yan, Y. Na, Q. Huang and X. Chen, *Appl. Phys. Lett*. 2011, **99**, 251905-251908.

18 B. Fu and L. Gao, *Scripta Materialia* 2006, **55**, 521-524.

19 E. O. Chi, W. S. Kim and N. H. Hur, *Solid state commun*. 2001, **120**, 307-310.

20 K. Takenaka, A. Ozawa, T. Shibayama, N. Kaneko, T. Oe and C. Urano, *Appl. Phys. Lett*. 2011, **98**, 022103-022105.

21 S. Isaji, Y. Bin and M. Matsuo, *Polymer*. 2009. **50**, 1046-1053.

22 C. T. Avedisian, R. E. Cavicchi, P. M. McEuen, X. Zhou, W. S. Hurst and J. T. Hodges, *Appl. Phys. Lett*. 2008, **93**, 252108-252110.

23 H. C. Neitzert, L. Vertuccio and A. Sorrentino, *IEEE Trans. on Nanotechnol*. 2011, **10**, 688-693.

24 K. Chu, D. Kim, Y. Sohn, S. Lee, C. Moon and S. Park, *IEEE Electron Device Letters*, 2013, **34**, 668-670.

25 **M.** Mohiuddin and S. Van-Hoa, *Nanoscale Res. Lett.* 2011, **6**, 419-423

26 A. D. Bartolomeo, M. Sarno, F. Giubileo, C. Altavilla, L. Iemmo, S. Piano, F. Bobba, M. Longobardi, A. Scarfato, D. Sannino, A. M. Cucolo and P. Ciambelli, *J. Appl. Phys*. 2009, **105**, 064518-064526.

27 H. Jiang, B. Liu, Y. Huang and K. C. Hwang, *J. Eng. Mat. Tech*. **2004**, *126*, 265-270.

28 F. Y. Wu and H. M. Cheng, J. Phys. D: Appl. Phys. 2005, 38, 4302–4307

29 P. Sheng, *Phys. Rev. B*. 1980, **21**, 2180-2195.

30 C. A. Hewitt, A. B. Kaiser, S. Roth, M. Craps, R. Czerw and D. L. Carroll, *Appl. Phys. Lett*. 2011, **98**, 183110-183112.

31 G.-T. Kim and E.-S. Park, *J. Appl. Polym. Sci*. 2008, **109**, 1381-1387.

32 P. Thielemann, D. J. Yun, P. Asbeck, P. R. Bandaru and S. H. Park, *Organic Electronics*. 2013, **12**, 1531-1537

33 Y. A. Kim, T. Hayashi, Y. Fukai, M. Endo, T. Yanagisawa and M. S. Dresselhaus, Chemical Physics Letters. 2002, 355, 279–284

34 L. Forró, R. Gaal, C. Grimaldi, M. Mionić, P. R. Ribič, R. Smajda and A. Magrez, AIP Advances, 2013, 3, 092117-7

35 I. D. Rosca, S. V. Hoa, Carbon, 2009, 47, 1958-1968

36 D. Cui, Q. Liu and F. Chen, *J. Power Sources*. 2010, **195**, 4160-4167.

37 D. Cui, C. Yang, K. Huang and F. Chen, *Int. J. Hydrogen. Energ*. 2010, **35**, 10495-10504.

38 K. Kazymyrenko and X. Waintal, *Phys. Rev. B*. 2008, **77**, 115119-115125.